ISSN 0023-1584, Kinetics and Catalysis, 2011, Vol. 52, No. 5, pp. 659–671. © Pleiades Publishing, Ltd., 2011.
Original Russian Text © D.E. Zavelev, M.V. Tsodikov, G.M. Zhidomirov, R.A. Kozlovskii, 2011, published in Kinetika i Kataliz, 2011, Vol. 52, No. 5, pp. 675–687.

Role of the Surface Hydroxyl Groups of Modified Titanium Oxide in Catalytic Ethylene Oxide Hydration

D. E. Zavelev[a], **M. V. Tsodikov**[a], **G. M. Zhidomirov**[b, c], **and R. A. Kozlovskii**[d]
[a] *Topchiev Institute of Petrochemical Synthesis, Russian Academy of Sciences, Moscow, 119991 Russia*
[b] *Boreskov Institute of Catalysis, Siberian Branch, Russian Academy of Sciences, Novosibirsk, 630090 Russia*
[c] *Zelinsky Institute of Organic Chemistry, Russian Academy of Sciences, Moscow, 119991 Russia*
[d] *Mendeleev University of Chemical Technology of Russia, Moscow, 125047 Russia*
e-mail: metalian@ips.ac.ru

Received October 12, 2010

Abstract—A quantum-chemical study of the mechanism of ethylene oxide hydration on titanium oxide (anatase) modified with phosphorus additives was performed. It was demonstrated that the hydroxyl groups of the anatase surface are of importance for the activation interaction of ethylene oxide with the catalyst surface. The activation of the ethylene oxide molecule and proton transfer occur with the participation of these hydroxyl groups. It was found that the modification of the titanium oxide surface with phosphorus additives plays a crucial role in proton transfer.

DOI: 10.1134/S0023158411050193

INTRODUCTION

The addition reactions of α-oxides, in particular, ethylene oxide, and substances with a labile hydrogen atom form the basis of a number of large-scale processes of basic organic synthesis. The products of such processes are glycols, cellosolves, carbitols, nonionic surfactants, and polyethers. As a rule, these reactions are carried out under homogeneous conditions without a catalyst or under conditions of acid or alkaline catalysis [1–3].

The addition of ethylene oxide is a consecutive–parallel reaction, which proceeds according to the following scheme:

$$\mathrm{XOH} \xrightarrow[k_0]{\mathrm{C_2H_4O}} \mathrm{XOCH_2CH_2OH}$$

$$\xrightarrow[k_1]{\mathrm{C_2H_4O}} \mathrm{XOCH_2CH_2OCH_2CH_2OH} \xrightarrow[k_2]{\mathrm{C_2H_4O}} \ldots,$$

where X = Alk, Ar, R–C(O), or H.

If X = H, the reagent is water, and the hydration of ethylene oxide is an industrial process for the production of ethylene glycol.

The composition of the reaction products and, consequently, the selectivity depend on the ratio of the rate constants of consecutive reactions to the rate constant of the first step of ethoxylation, which is referred to as a distribution coefficient [1, 4]: $S_i = k_i/k_0$.

The main problems with the use of homogeneous catalysts are insufficient selectivity for the formation of an oxide monoaddition product (thus, $S_1 \approx S_2 \approx \ldots \approx S_i \approx 1$ for acid catalysts [5] and $S_1 \approx 2$ and $S_2 \approx 3$ for basic catalysts [6, 7]) and high energy consumptions for the separation of a homogeneous catalyst from products and also for the separation of final reaction mixture components. Thus, for instance, a molar ratio of 1 : 12 between ethylene oxide and water is used to provide economically acceptable selectivity for the formation of ethylene glycol; this requires large power consumption for the evaporation of an excess of water during the isolation of the target product.

The application of heterogeneous catalysts removes the problem of catalyst separation from the reaction products (active centers are immobilized on the support surface) and substantially increases the selectivity of the process [8–10], which makes it possible to use a smaller excess of the second reagent (water in the case of hydration) and to decrease separation expenditures.

Use of catalysts with a uniform pore distribution is the most effective method for further increasing the selectivity. It sharply decreases the formation of products with the degree of ethoxylation higher than a specified value; that is, a sieve effect occurs in the course of reaction [11]. Phosphorus–titanate oxides prepared by an alcoxo method can be used as such catalysts [11]. These systems are single-phase polycrystalline mixed oxides with the empirical formula $P_xTi_{1-0.5x}O_{2\pm\delta}$, where $x = 0.01$–0.03. They possess a highly organized structure with a uniform porosity and exhibit membrane properties; that is, they are permeable to gas reagents; they also exhibit molecular-sieve properties in the ethoxylation reactions of alcohols [12, 13].

However, the molecular reaction mechanism was not analyzed in previous studies [11, 13]. A reasonable hypothesis could be that the strong aprotic acid sites of titanate oxides mainly participate in the limiting stage

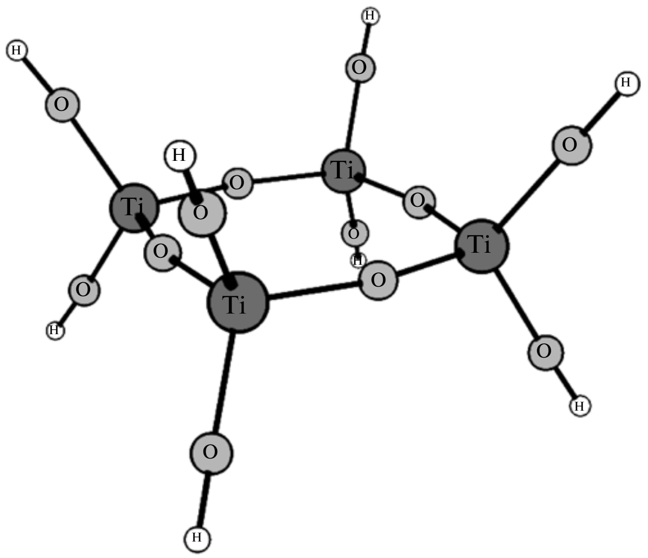

Fig. 1. The smallest possible cluster that simulates the (001) surface of anatase.

of ethoxylation, whereas the basic sites activate alcohol groups to provide concerted acid–base catalysis on the catalyst surface. On the basis of this hypothesis, the following reaction scheme was proposed for the activation of reagents [11] (it is believed that, in this case, the structure of the activated complex is analogous to that accepted for the cycloaddition reactions of carbon dioxide and epoxies [14]):

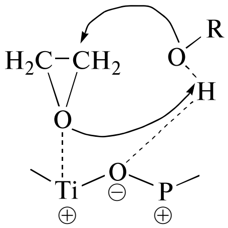

(I)

An increase in the positive charge on titanium atoms after the surface modification of anatase with phosphorus-containing compounds, which was noted previously [11], makes in favor of the assumed coordination of reagents. In this case, Teleshev et al. [15] found that the oxidation state of phosphorus and the activity of the resulting catalytic system depend on the precursor chosen. Gansaüer et al. [16] studied such a coordination of epoxies to the titanium atom (in titanocene complexes).

At the same time, a reaction mechanism that implies the active participation of surface hydroxyl or alkoxide groups can be considered. In particular, Di Serio with coauthors [17, 18] discussed the possibility of activating ethylene oxide (in catalysis with an aluminum alkoxide–sulfate catalyst) according to the following reaction scheme:

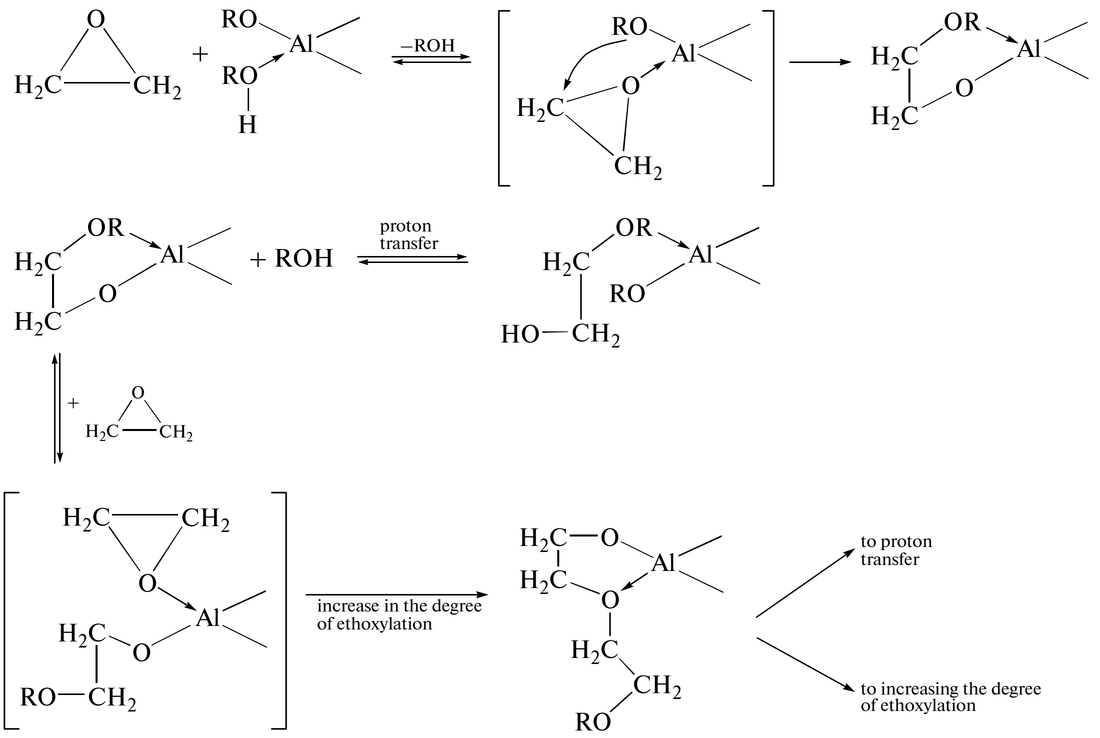

(II)

Maihom et al. [19] theoretically studied an analogous reaction scheme as applied to the hydration of ethylene oxide on zeolites H-ZSM-5. They also considered the single-stage mechanism of ethylene oxide hydration on zeolites H-ZSM-5 with the following reaction scheme of activation:

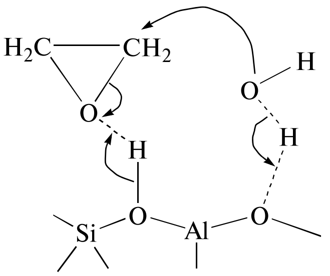

(III)

In this work, which is the first part of a quantum-chemical study of the reaction mechanism of the addition of ethylene oxide to substances with a labile hydrogen atom in the presence of phosphorus–titanate catalysts, we consider the simplest model example of this reaction, namely, the process of ethylene oxide hydration.

COMPUTATIONAL DETAILS

The calculations were performed according to the Firefly program package [20] within the framework of density functional theory (DFT) [21] with the use of a hybrid functional with gradient corrections according to Becke [22, 23], the Lee–Young–Parr correlation functional [24] (B3LYP functional), and the 6-31G ** basis set [25–28]. The SBKJC effective potential and associated basis set [29–31] were used in the calculations of clusters containing four titanium atoms . Charges on atoms were calculated by the Hirshfeld method [32] using the NBO program, version 5.0 [33].

The results of the calculations were visualized with the use of the ChemCraft program package [34].

The examination was conducted for the most representative (001) surface of an anatase crystal [35]. In accordance with this, in the discussion of the immobilization of phosphorus, a structural fragment of the oxide surface as a cluster containing four titanium atoms linked by oxygen atoms was chosen. The dangling bonds of titanium atoms were saturated with hydroxyl groups, as is customary in cluster calculations of this kind [36] (Fig. 1). At first glance, an obvious disadvantage of this cluster simulation of a surface layer fragment of anatase is a decrease in the coordination number of an oxygen environment of titanium atoms, as compared with their environment in the oxide. The existing experience in similar simulations [36] makes it possible to conclude that the main danger here consists in the possible overestimation of the accessibility of surface active centers to reagents rather than in a change in the energy of surface interactions. The former, in principle, can be considered in the consideration of particular reaction paths on the surface. On the other hand, published data suggest that the surface relaxation of oxides, in particular, anatase [37], can cause an effective decrease in the coordination number of titanium atoms.

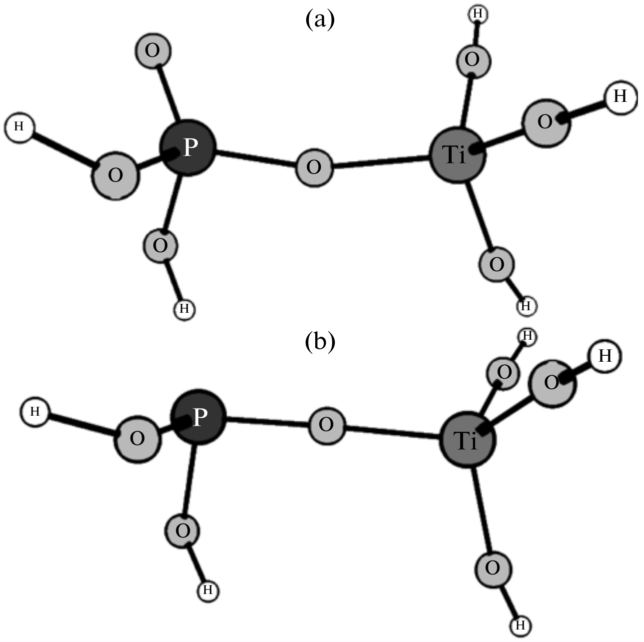

Fig. 2. Minimum clusters for the simulation of the ethoxylation reaction: (a) with the pentavalent P atom and (b) with the trivalent P atom.

For the ethoxylation reaction mechanism's simulation, we decreased the model cluster to one titanium atom linked to a pentavalent phosphorus atom through an oxygen bridge (Fig. 2a). For comparison, we also constructed a structure with a trivalent phosphorus atom (Fig. 2b).

Then, we optimized the structure of the coordination complex of a catalyst with ethylene oxide and water molecules after the optimization of the geometry of model clusters and calculated transition states at the elementary steps of the reaction. These latter were tested for the presence of a corresponding imaginary frequency in the spectrum of the harmonic oscillations of the transition structure and checked for the correspondence to reagents and products along the reaction coordinate. When it was impossible to determine the structure of the transition state, we calculated an energy profile along the selected reaction coordinate in order to obtain the upper estimate of the activation energy of the given elementary step of the reaction.

EXPERIMENTAL

For some samples of phosphorus–titanate catalysts for ethoxylation prepared on the basis of different precursors previously [11], IR absorption spectra were recorded (KBr pellets, 4000–400 cm^{-1}, Bruker IFS 66-v-s).

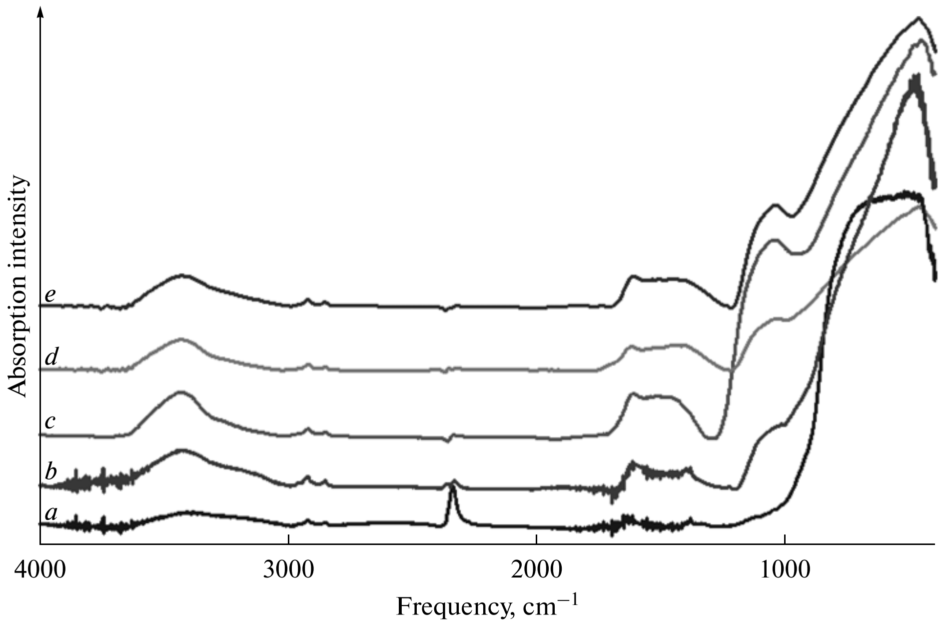

Fig. 3. IR absorption spectra of (*a*) an anatase sample prepared by an alcoxo method and analogous samples modified with phosphorus with the use of (*b*) ethryol phosphite (3% P), (*c*) ethryol phosphite (6% P), (*d*) 2-diamido-4-methyl-1,2,3- dioxaphosphorinane (3% P), and (*e*) diethylamino(2,2'-dioxa-5,5'-dimethyl-1,1'-diphenylmethano)phosphocane (3% P) as precursors.

RESULTS AND DISCUSSION

IR Spectroscopic Studies

Figure 3 shows the Fourier transform IR spectra of pure anatase prepared by the alcoxo method and the samples whose precursors were ethryol phosphite (phosphorus content of 3 wt %), ethryol phosphite (phosphorus content of 6 wt %), 2-diamido-4-methyl-1,2,3- dioxaphosphorinane (phosphorus content of 3 wt %), and diethylamino(2,2'-dioxa-5,5'-dimethyl-1,1'-diphenylmethano)phosphocane (phosphorus content of 3 wt %).

The most pronounced distinction of the spectra of the samples modified with phosphorus is the presence of a clearly defined shoulder in the region of 1050–1150 cm^{-1}, which can correspond to the P=O bond, although its frequency is smaller than the vibrational frequencies characteristic of the P=O double bond [38, 39]. This frequency is more characteristic of the P=O bond having a hydrogen bond [39]. On the other hand, published data concerning anatase modified with phosphorus suggest either the absence of phosphoryl oxygen in a pure form and the possible assignment of this shoulder to a phosphate structure [40–44] or a shift of the band due to P=O bond vibrations under the action of surface Ti–O bonds [45]. Körösi et al. [46] reported the possible interaction of hydroxyl groups on the surface of anatase with phosphate anions to form crosslinks. Thus, either a phosphate structure (with monodentate or bidentate immobilization) is formed or a hydrogen bond appears between the phosphoryl oxygen and the hydrogen of surface hydroxyl.

Note that, with the use of the same precursor, an increase in absorption in the above region corresponded to an increase in the phosphorus content of the sample. However, the intensities of the test shoulders were different in the spectra of samples with the same phosphorus content prepared from different precursors; this may suggest that a portion of phosphorus does not participate in the formation of structures containing phosphoryl oxygen during immobilization. Different catalytic activity of samples with the same phosphorus content [11] seems to confirm this conclusion; however, the very low activity of the samples obtained from ethryol phosphite [11], in spectra of which the above shoulder is clearly pronounced, cannot be explained.

On the other hand, Bhaumik and Inagaki [47] believed that the shoulder in this region (1000–1050 cm^{-1}) corresponds to Ti–O–P lattice vibrations. Note that the samples prepared from ethryol phosphite are characterized by a decrease in the absorption in this region, as compared with the samples based on other precursors; this can also suggest the dependence of phosphorus immobilization on the nature of a precursor.

In the spectra of phosphorus-containing samples, an increase in absorbance in the region of 900–1000 cm^{-1}, which, probably, corresponds to the deformation vibrations of P–O–H bonds, can also be noted, as compared with the spectrum of pure anatase [41, 48]. It is likely that the stretching vibrations of the P–O–P bond also occur in this region [48, 49]; however, the resolving power of the instrument used was found insufficient for recognizing them. In this case, absorption bands corresponding to P–H bonds (the range of

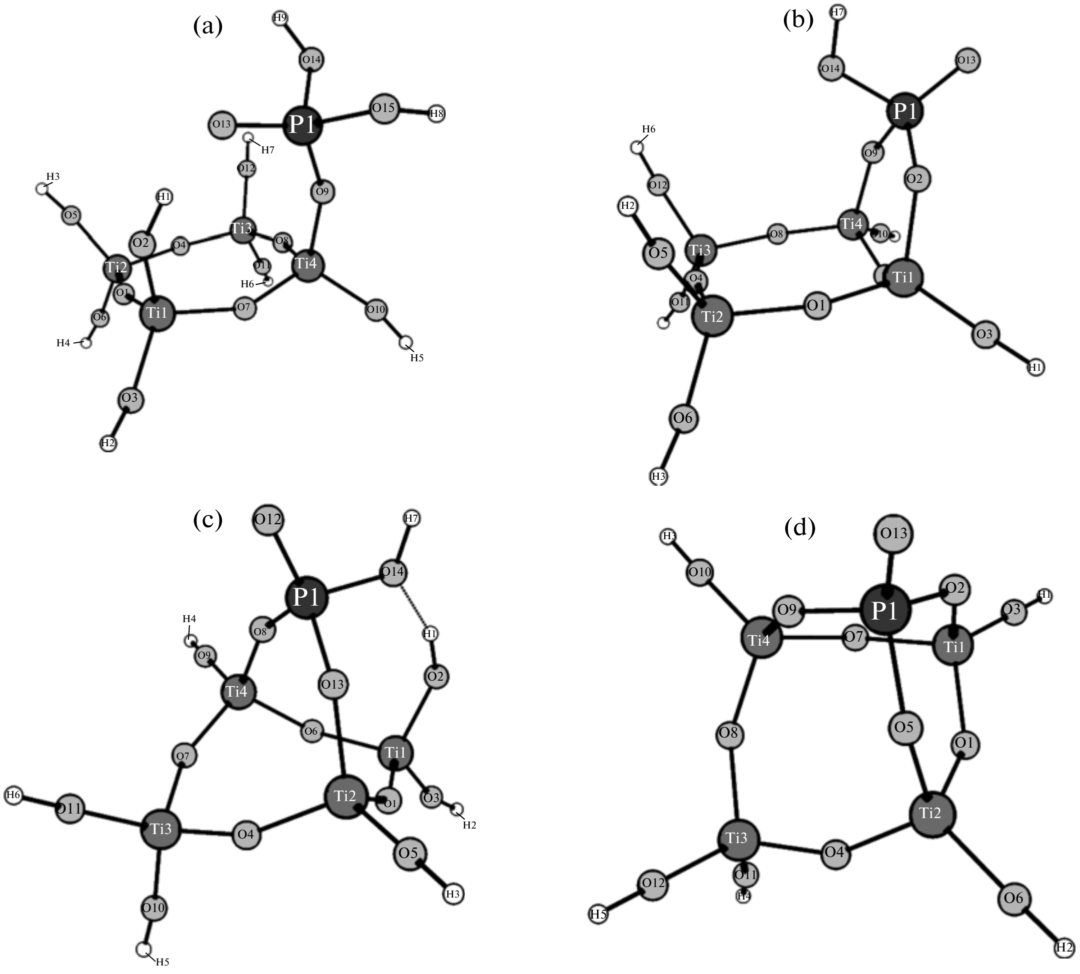

Fig. 4. Possible versions of the immobilization of the phosphorus atom on the (001) surface of anatase. Immobilization energies, kcal/mol: (a) –14.6, (b) 1.1, (c) –6.5, and (d) 15.3.

2440–2350 cm^{-1}) were absent from the spectra [39]; this is expectable based on the structure of precursors.

The above spectra clearly exhibit a number of lines in the range of 3600–3900 cm^{-1}, which correspond to the vibrations of OH groups [50]. Because the samples were calcined both immediately after preparation and before the measurement of spectra, we can conclude that these bands belong to the remaining surface OH groups (it is well known that water can be adsorbed on the surface of pure anatase either as molecules or dissociatively as a hydroxyl cover [50–55]).

A shoulder in the region of 1600–1700 cm^{-1}, which is characteristic of the deformation vibrations of water molecules, was present in both spectra. Busca and coauthors [56, 57] assigned absorption in the above range (in the spectra of zirconium phosphates partially dehydrated in a vacuum and vanadium(II) hydroorthophosphate hemihydrate) to the deformation vibrations of water molecules adsorbed molecularly on the surface of oxides. Thus, the molecular adsorption of water also occurs on the surface of all of the test samples. It is well known [58] that the surface of anatase modified with phosphates is hydrophobic. It is likely that the inconsistency with the results obtained in this work can be explained by a lower concentration of grafted groups on the surface and by the use of the alcoxo method.

Immobilization of Phosphorus Atoms on the Anatase (001) Surface

Figure 4 shows the structures corresponding to local minimums in potential energy surfaces for the immobilization of P(V) atoms on the (001) surface of anatase. Similar structures were obtained for P(III); therefore, they are not represented in the figures. Immobilization energies for structures **a**–**d** with the P(V) atom are –14.6, 1.1, –6.5, and 15.3 kcal/mol, respectively, and they are –10.8, –3.2, –4.3, and 15.2 kcal/mol, respectively, for analogous structures with the P(III) atom. These values were found as differences between the total energies of the optimized structures of final and initial substances either in a substitution reaction (for an isomorphous case) or upon

Table 1. Hirshfeld charges (|e|) on titanium atoms in the initial cluster and clusters modified with phosphorus

Structure	Ti1	Ti2	Ti3	Ti4
Initial cluster (D4)	1.760	1.760	1.760	1.760
Modification with P(V), structure **a**	1.766	1.763	1.764	1.791
Modification with P(V), structure **b**	1.793	1.770	1.770	1.793
Modification with P(V), structure **c**	1.767	1.792	1.768	1.792
Modification with P(V), structure **d**	1.785	1.795	1.771	1.795
Modification with P(III), structure **a**	1.779	1.763	1.763	1.776
Modification with P(III), structure **b**	1.786	1.773	1.778	1.781
Modification with P(III), structure **c**	1.770	1.776	1.763	1.776
Modification with P(III), structure **d**	1.777	1.784	1.766	1.784

surface immobilization (for structures **a**–**d**); therefore, they cannot be considered as the thermochemically accurate. However, their ratio qualitatively shows that structure **a** is the most probable structure in both cases. At the same time, the formation of structure **c** is also possible for P(V) and the formation of structures **b** and **c** is possible for P(III). Differences in the energies of immobilization may be caused by at least two factors: the absence of anatase surface distortions upon the immobilization of phosphorus (for structure **a**) and additional structure stabilization because of the formation of a hydrogen bond between the hydroxyl groups of titanium and phosphorus (for structure **c**).

We also attempted to find a local minimum, which corresponds to the immobilization of phosphorus through two bridging oxygen atoms at one titanium atom, as this was assumed by Hadjiivanov et al. [58], who examined anatase modification with inorganic phosphates. However, we failed to find the local minimum that corresponds to this structure: in the course of geometry optimization, the system reached a minimum corresponding to structure **a**, which was mentioned above.

The version of the isomorphous replacement of Ti(IV)$(OH)_2$ by P(III)(OH) or P(V)$(OH)_3$ is extremely improbable because of a strong difference in the ionic radii. Calculations showed that the endothermicity of these replacements is 179 and 175 kcal/mol, respectively; that is, the impossibility of this version was demonstrated.

Table 1 summarizes the calculated charges on titanium atoms in the above structures. It can be seen that the introduction of phosphorus increases a positive charge on titanium atoms; however, this increase is not so considerable in comparison with that in pure anatase, and it primarily concerns the titanium atoms to which phosphorus was grafted. That is, the introduction of phosphorus noticeably influences the properties of only the nearest atoms of titanium.

Generally, charges on the protons of the hydroxyl groups of the surface of anatase also changed only slightly upon the introduction of P(V): from 0.505 in the initial cluster to 0.503–0.514 in the modified clusters. The exception is the proton that interacts with phosphoryl oxygen in structures **a** and **b**: the charge on it increases to 0.540 and 0.534, respectively, which is greater than that on the protons of hydroxyl groups at phosphorus (0.508–0.513 for structures **a** and **b**, 0.525 for structure **c**, and 0.513–0.517 for phosphoric acid).

An analogous behavior was observed upon the introduction of P(III): the charges on the protons of the hydroxyl groups of the surface of anatase varied from 0.504 to 0.511, except for a proton in the 2-position in structure **b** (a charge of 0.533), and interaction with the hydroxyl group of phosphorus occurred. In this case, the charges on the protons of the hydroxyl groups of phosphorus were 0.531 and 0.487 for structure **a**, 0.541 for structure **b**, and 0.527 for structure **c**.

Thus, in the most expected structures formed upon the introduction of P(V), the proton of the hydroxyl group of titanium is more acidic, while the proton of the hydroxyl group of phosphorus becomes more acidic upon the introduction of P(III).

The O–H bond length can be considered another characteristic of the acidity of various protons (Table 2). As can be seen, the maximum O–H bond length corresponds to the protons of the hydroxyl groups of the surface of anatase, which exhibit the greatest charge according to Hirshfeld; that is, both of the characteristics of acidity give similar results. As for the hydroxyl groups of phosphorus, in the case of P(V), the acidity of the protons of these groups is somewhat lower than that in the orthophosphoric acid molecule, and it is higher than that in this molecule and in $P(OH)_3$ in the case of P(III). Note that the calculated bond lengths differed from the experimental values as a result of the use of a narrow SBKJC basis set; however, general regularities are also manifested in this case.

Mechanism of Ethylene Oxide Hydration

First, we calculated the reaction path of uncatalyzed ethylene oxide hydration [1] and identified the transition state at the main step of the process (Fig. 5b). Then, descending along the reaction coordinate, we

Table 2. O–H bond lengths in the initial cluster and clusters modified with phosphorus

Structure	O–H bond length, Å		
	the longest bond at the Ti atom	the other bonds at the Ti atom	at the P atom
Initial cluster (D4)	0.976	0.976–0.976	–
H_3PO_4	–	–	0.998, 0.997, 0.995
Modification with P(V), structure **a**	1.017	0.977–0.979	0.997, 0.997
Modification with P(V), structure **b**	0.977	0.977–0.977	0.996
Modification with P(V), structure **c**	1.013	0.976–0.978	0.994
Modification with P(V), structure **d**	0.977	0.977–0.977	–
$P(OH)_3$	–	–	0.999, 0.999, 0.994
Modification with P(III), structure **a**	0.987	0.977–0.977	1.029, 1.001
Modification with P(III), structure **b**	1.027	0.976–0.986	1.038
Modification with P(III), structure **c**	0.985	0.976–0.977	1.030
Modification with P(III), structure **d**	0.977	0.976–0.977	–

revealed the prereaction complex (Fig. 5a) and the postreaction complex (Fig. 5c). Two water molecules participate in this process; one of them forms the H_1–O_2 hydrogen bond with the oxygen atom of ethylene oxide and the second forms a hydrogen bond with the former. In the transition state, the C_1–O_2 bond is weakened; in this case, the C_1–O_3 bond is conceived. The found transition state is characterized by one imaginary frequency of 455 cm^{-1} in the calculated vibrational spectrum; this frequency corresponds to the vibrations of C_1–O_2, C_1–O_3, H_6–O_1, and H_1–O_2 bonds. In the path from the transition state to the postreaction complex, the final breaking of the C_1–O_2 bond occurs and C_1–O_3 and H_1–O_2 bonds are formed, whereas the H_6–O_3 and H_1–O_1 bonds become hydrogen bonds. The postreaction complex is the coordination complex of ethylene glycol and water.

The activation energy of the reaction that occurs by this mechanism is 50.7 kcal/mol; in this case, the energies of coordination adsorption in the prereaction and postreaction complexes are –19.9 and –15.9 kcal/mol, respectively.

Based on reaction scheme (I), which describes the activation of reagents on the phosphorus–titanate catalysts as a first approximation for the transition state of the reaction, we proposed a two-step reaction scheme. It includes the transition of the coordination complex of the catalyst with ethylene oxide to an intermediate and the subsequent proton transfer with the formation of the postreaction complex; that is, in principle, reaction scheme (I) is reduced to reaction scheme (II).

Figure 6 shows the prereaction coordination complex, the transition state corresponding to the first step of the reaction, and the bidentate intermediate for the system with P(V). The energy of coordination adsorption was –35.1 kcal/mol, the activation energy was 48.2 kcal/mol, and the energy of transition from coordination adsorption to dissociative adsorption was –23.8 kcal/mol. The analysis of the harmonic vibration frequencies of the structure that corresponds to the transition state gives an imaginary frequency of 516 cm^{-1} for the vibrations of C_2–O_8 and C_2–O_3 bonds.

Note that we also examined the prereaction complex that strictly corresponds to reaction scheme (I); that is, it implies the coordination of the water molecule to bridging oxygen rather than the hydroxyl group at the phosphorus atom. However, it turned out that its energy level is higher by 11.1 kcal/mol than that of the complex represented in Fig. 6a. Because the water molecule does not directly participate in the transition from coordination adsorption to dissociative adsorption, it is likely that the energy parameters in this case are close to those corresponding to the previous case.

We also calculated analogous structures for the system with P(III): the energy of coordination adsorption was –28.2 kcal/mol, the activation energy was 44.9 kcal/mol, and the energy of transition from coordination adsorption to dissociative adsorption was –19.1 kcal/mol. The analysis of the harmonic vibration frequencies of the structure corresponding to the transition state gives an imaginary frequency of 503 cm^{-1} for vibrations analogous to those described above. The energy level of the prereaction complex corresponding to reaction scheme (I) is higher by 6.0 kcal/mol.

The structures of the transition states are similar to the structures described in the literature [17–19].

We also attempted to calculate the prereaction coordination complex of the ethylene oxide molecule with the phosphorus atom (for the system with P(V), in which a charge on the phosphorus atom is obviously higher). However, the geometry optimization led us to the conclusion that this molecule should be coordinated to the titanium atom. Analogous attempts to describe a bidentate intermediate with the phosphorus atom were also unsuccessful.

For the step of proton transfer, a transition state corresponding to reaction scheme (IV) with an activation energy of 57.0 kcal/mol was found.

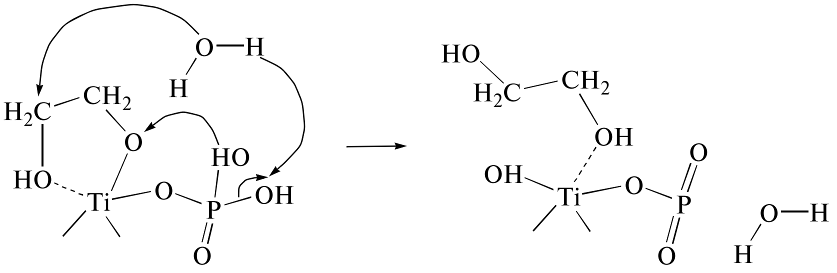

(IV)

An analogous reaction path was also calculated for the system with P(III), and the activation energy was 45.5 kcal/mol.

The occurrence of this reaction path at the final step of the reaction is improbable because of the high activation energy. This can be easily explained considering that the above reaction path includes the processes of the degradation of the bidentate intermediate, which is comparatively stable, as noted above, and the formation of the second phosphoryl oxygen atom.

Therefore, we considered the other reaction path with the retention of the intermediate:

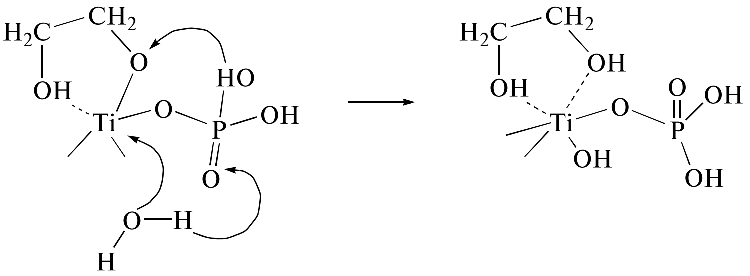

(V)

We failed to find a transition state for this reaction path; therefore, we calculated the energy profile of the reaction transition in which the length of the H–O bond formed between a proton of the water molecule and the phosphoryl oxygen changes with the optimization of the geometry of the entire remaining structure. The results of the calculation allowed us to conclude that a considerable activation barrier is absent from this reaction path (it is lower than 5 kcal/mol). The step itself is slightly endothermic; its activation energy is close to the thermal effect (5.8 kcal/mol), which complicates the localization of the transition state.

Obviously, this proton transfer mode can occur only in the system containing P(V) because, in this case, the phosphoryl oxygen atom plays an active role. At the same time, we can also examine a similar mechanism for P(III), which includes the intermediate participation of the hydroxyl group at the phosphorus atom:

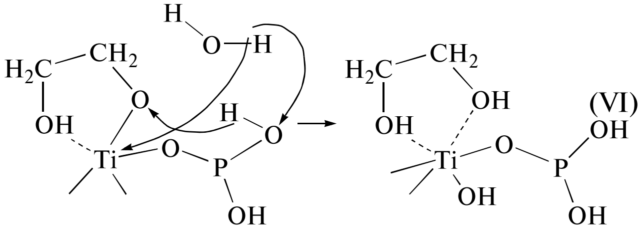

(VI)

The activation energy of the transition state for this reaction path is 3.5 kcal/mol.

The calculated activation energies for the first step of the discussed mechanism and the uncatalyzed reaction are sufficiently close to each other; based on the experimental data, a more effective catalytic reaction path should be found. Therefore, we considered a single-step reaction path corresponding to reaction scheme (III) for the system with P(V). Figure 7 shows the prereaction complex, the transition state, and the postreaction complex for this path. In this case, the activation energy of the reaction was 24.8 kcal/mol, the energy of the coordination adsorption of reagents was –34.4 kcal/mol, and the energy of the coordination adsorption of the product was –16.7 kcal/mol. The reaction occurs by a synchronous mechanism (S_N2): ethylene oxide coordinated to the proton of an OH group on the catalyst surface (by the O_8–H_1 hydrogen bond) is activated because of this coordination, and the C_1–O_8 bond is ruptured synchronously with a nucleophilic attack of the water molecule on the C_1 atom to cause the formation of the C_1–O_9 bond. In this case, synchronous proton transfer occurs: the O_1–H_1 bond is ruptured and the O_8–H_1 bond is formed, the O_6–H_4 bond is ruptured and the O_1–H_4 bond is formed, and the O_9–H_{10} bond is ruptured and the O_5–H_{10} is formed. Thus, a catalytic cycle is closed. An imaginary frequency of 418 cm^{-1}, which corresponds to the vibrations of all of the above ruptured and formed bonds, corresponds to the described transition state in the calculated vibrational spectrum. The phosphoryl oxygen atom participates in proton transfer; this fact can explain the catalytic activity of the system containing P(V). Obviously, proton transfer cannot take place in the case of modification with P(III).

We also attempted to describe the prereaction complexes with the coordination of ethylene oxide to the hydroxyl group of phosphorus. For the system containing P(V), we found the structures shown in Fig. 8: the prereaction complex, the transition state, and the postreaction complex. The activation energy was 59.6 kcal/mol, the energy of the coordination adsorption of reagents was –23.7 kcal/mol, and the and energy of the coordination adsorption of the product was –23.1 kcal/mol. An imaginary frequency of 516 cm^{-1} for the vibrations of all of the formed and broken bonds corresponds to the transition state in the calculated vibrational spectrum. The postreaction complex corresponds to the adsorption of formaldehyde hemiacetal and methanol on the catalyst. Taking into account the found activation energy (as compared with the most energetically advantageous version), we can conclude that this reaction path is extremely improbable for this system.

We failed to reveal an absolutely analogous reaction path for the system with P(III); however, we managed to find two similar reaction paths, in which ethylene oxide is coordinated to the hydroxyl group of phosphorus:

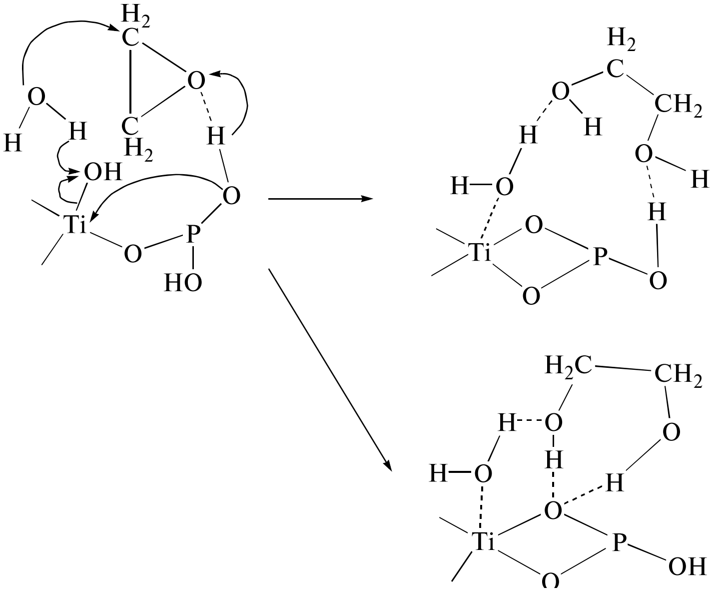

(VII)

The activation energies for the first and second variants were 46.4 and 44.5 kcal/mol, respectively; the energy of the coordination adsorption of the reagents was –23.0 kcal/mol, and the energies of the coordination adsorption of the product were –23.3 and –20.4 kcal/mol, respectively. These transition states correspond to an imaginary frequency of –442 or –448 cm^{-1}, respectively, for the vibrations of all of the formed and ruptured bonds in the calculated vibrational spectra. The postreaction complex corresponds to the adsorption of ethylene glycol on the catalyst with removed water molecules. Obviously, this version cannot occur because of the high activation energy. Note that we also failed to find a similar reaction path for the system with P(V).

A comparison of the found activation energies led us to the conclusion that anatase modified with P(V) possesses clearly pronounced catalytic properties. The reaction of ethylene oxide hydration mainly occurs by the S_N2 mechanism, and it is accompanied to an insignificant degree by an uncatalyzed reaction and a reaction occurring by a two-step mechanism through the formation of a bidentate intermediate. However, anatase modified with P(III) does not exhibit pronounced catalytic properties. Thus, the previously published kinetic data [11] are confirmed.

Thus, we theoretically studied the reaction of ethylene oxide hydration on the surface of anatase modified with phosphorus. We studied the Fourier transform IR absorption spectra and made a conclusion on the presence of hydroxyl groups and molecularly adsorbed water on the surfaces of pure and modified anatase. We analyzed various versions of phosphorus immobilization on the surface of titanium oxide; the replacement of hydrogen in hydroxyl groups by the phosphoryl group should be considered most likely. We found that this replacement increases the acidity of protons in the hydroxyl groups of the surface of ana-

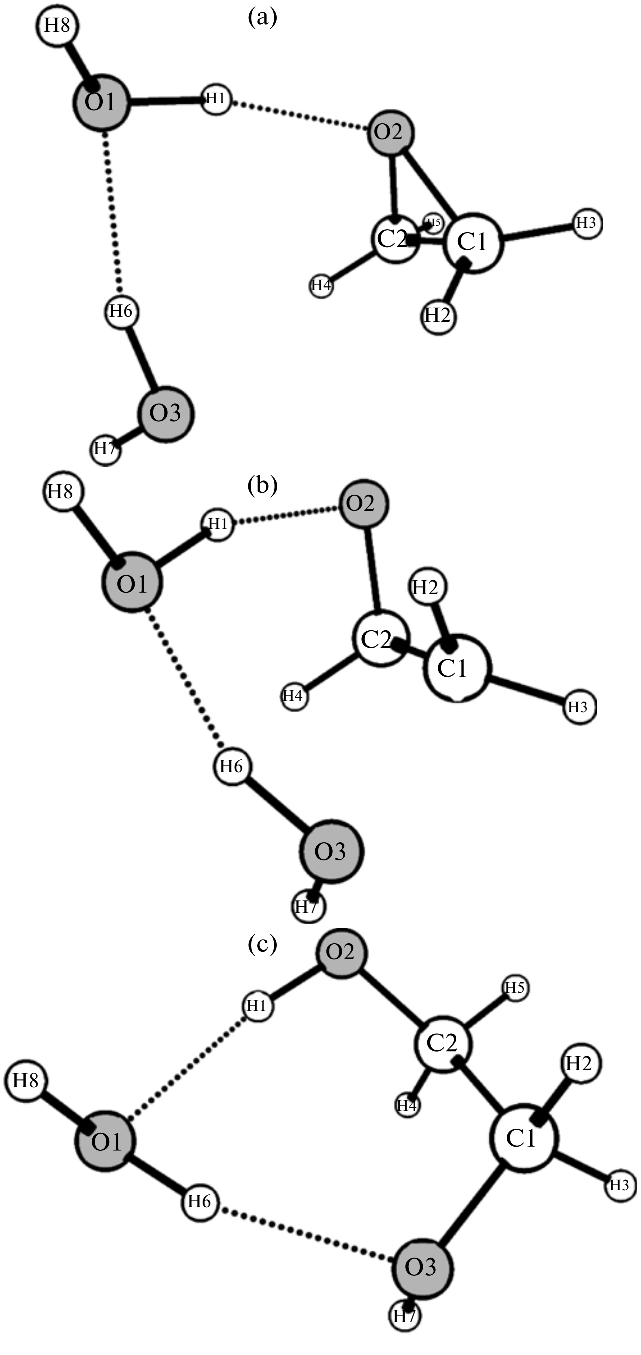

Fig. 5. (a) Prereaction complex, (b) transition state, and (c) postreaction complex in the uncatalyzed reaction of ethylene oxide hydration.

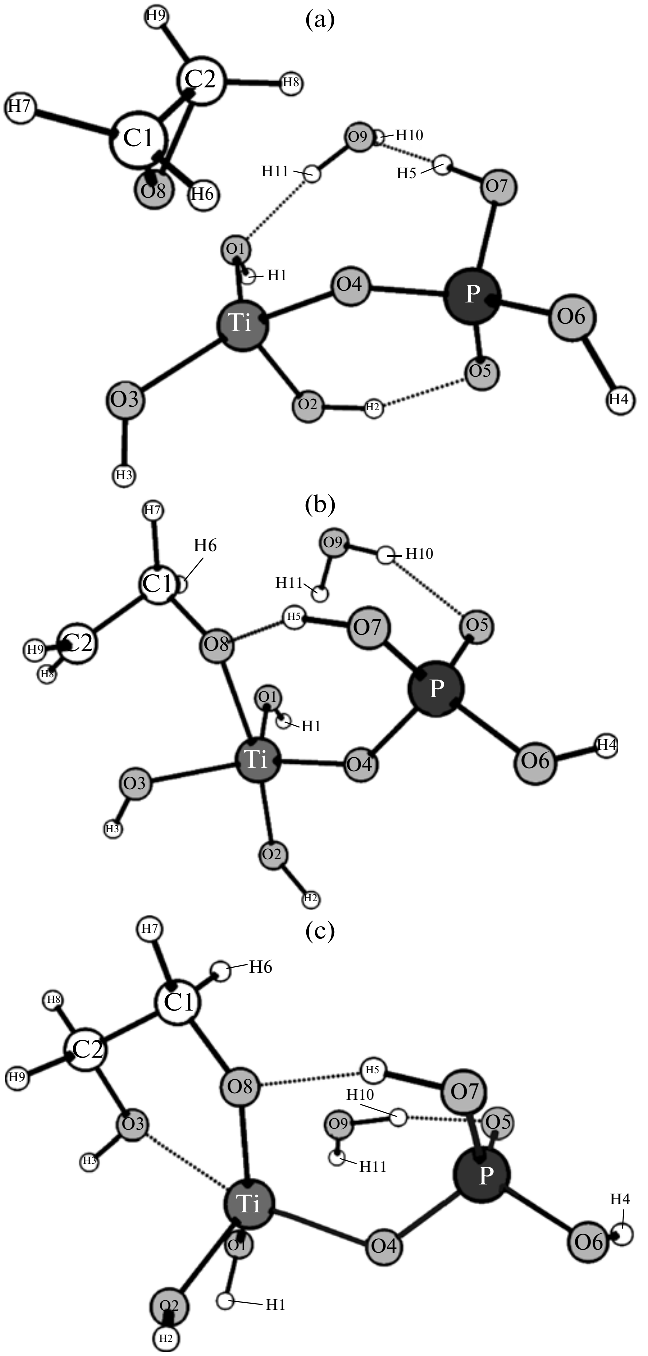

Fig. 6. (a) Prereaction complex, (b) transition state at the first step, and (c) intermediate in the two-step reaction of ethylene oxide hydration on the catalyst $P(V)_{0.07}Ti_{0.94}O_{2-\delta}$.

tase, whereas the acidity of surface Lewis acid sites changes insignificantly and the introduction of phosphorus has an effect only on the nearest atoms of titanium. We examined two initial adsorption states of ethylene oxide on the surface of TiO_2: with the coordination of epoxide oxygen to the titanium atom and to the hydrogen atom of the hydroxyl group, respectively. In the former case, the initial step of reaction consists in the opening of an epoxy ring with the transfer of the hydroxyl group from titanium oxide to an epoxide carbon atom and the coordination of the other carbon atom to the titanium atom by means of an oxygen bridge. As a result, a bidentate intermediate is formed, which is converted into the reaction product at the second step of the reaction, which is the catalytic dissociation of the water molecule. As a result of this, the entire catalytic cycle is closed. We found the efficient reaction paths of the dissociative addition of water

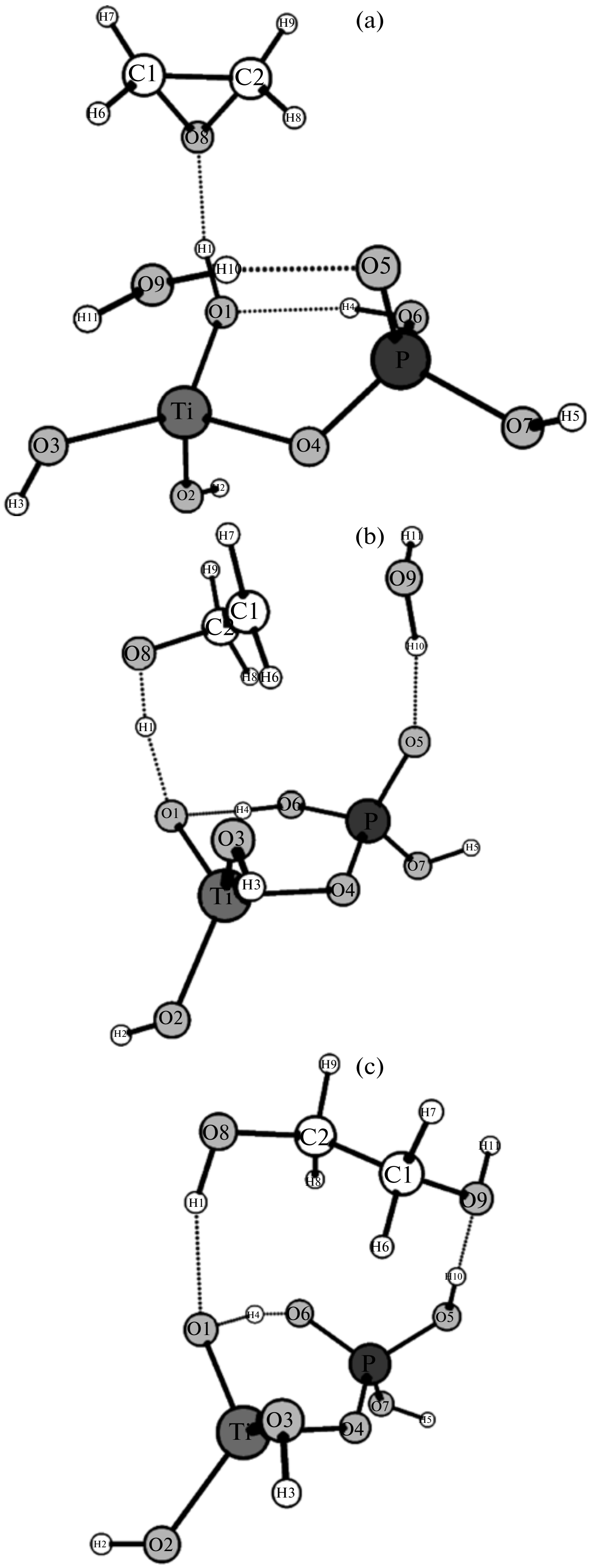

Fig. 7. (a) Prereaction complex, (b) transition state, and (c) postreaction complex in the single-step reaction of ethylene oxide hydration on the catalyst $P(V)_{0.07}Ti_{0.94}O_{2-\delta}$.

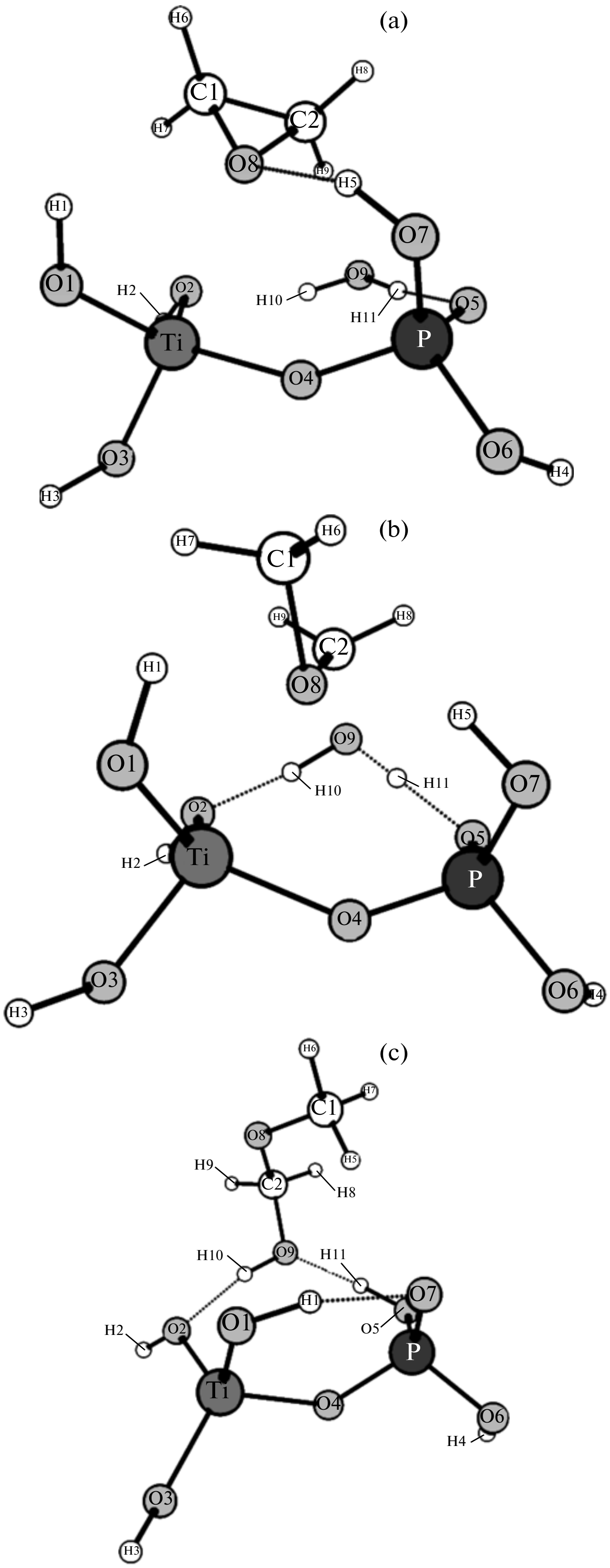

Fig. 8. (a) Prereaction complex, (b) transition state, and (c) postreaction complex in the course of ethylene oxide ring opening at the C–C bond on the catalyst $P(V)_{0.07}Ti_{0.94}O_{2-\delta}$.

molecules to the reaction complex in the cases of the immobilization of P(V) and P(III). Although, according to our estimations, the formation of a bidentate intermediate requires a sufficiently high activation energy, this reaction path deserves special attention because the formation of the intermediate is a sufficiently exothermal process. Nevertheless, we consider the priority reaction path that occurs by the S_N2 mechanism and implies the initial coordination of epoxide to the hydrogen of the hydroxyl group titanium oxide followed by an attack of the oxygen of the water molecule on the epoxide carbon. The single-step process of the catalytic conversion described in this work is characterized by a noticeably lower activation energy. It can occur only in the case of P(V) immobilization, which is qualitatively consistent with the experimentally observed noticeably higher catalytic activity of the system with P(V), as compared with the activity of the system with P(III) [11].

ACKNOWLEDGMENTS

We are grateful to Dr. Sci. (Chem.) G.N. Bondarenko, Cand. Sci. (Chem.) Yu.V. Kostina (Topchiev Institute of Petrochemical Synthesis, Russian Academy of Sciences), and Cand. Sci. (Chem.) G.A. Zhurko (Ivanovo State University of Chemical Technology). This work was supported by the Russian Foundation for Basic Research (project no. 09-03-00133-a) and the Russian Scientific School (project no. NSh-65264.2010.3).

REFERENCES

1. Lebedev, N.N., *Khimiya i tekhnologiya osnovnogo organicheskogo i neftekhimicheskogo sinteza* (Basic Organic and Petrochemical Syntheses: Chemistry and Technology), Moscow: Khimiya, 1988, 4th ed.
2. Dyment, O.N., Kazanskii, K.S., and Miroshnikov, A.M., *Glikoli i drugie proizvodnye okisei etilena i propilena* (Glycols and Other Ethylene Oxide and Propylene Oxide Derivatives), Moscow: Khimiya, 1976.
3. Manolova, N., Libiszowski, J., Szumanski, R., and Penszek, S., *Polym. Int.*, 1995, vol. 36, p. 23.
4. Shvets, V.F., *Doctoral (Chem.) Dissertation*, Moscow: Moscow Inst. of Chemical Technology, 1974.
5. Van Os, N.M., *Nonionic Surfactants*, Surfactant Science Series, vol. 72, New York: Marcel Dekker, 1998, p. 22.
6. Lebedev, N.N., Savel'yanov, V.P., and Baranov, Yu.I., *Zh. Prikl. Khim.*, 1969, vol. 42, p. 1815.
7. Van Os, N.M., *Nonionic Surfactants*, Surfactant Science Series, vol. 72, New York: Marcel Dekker, 1998, p. 5.
8. Makarov, M.G., *Doctoral (Chem.) Dissertation*, Moscow: Moscow Inst. of Chemical Technology, 1987.
9. Kustov, A.V., *Cand. Sci. (Chem.) Dissertation,* Moscow: Moscow Inst. of Chemical Technology, 1987.
10. Kozlovskii, I.A., *Cand. Sci. (Chem.) Dissertation*, Moscow: Mendeleev Univ. of Chemical Technology of Russia, 2003.
11. Kozlovskii, R.A., Yushchenko, V.V., Kitaev, L.E., Bukhtenko, O.V., Voloshchuk, A.M., Vasil'eva, L.N., and Tsodikov, M.V., *Izv. Akad. Nauk, Ser. Khim.*, 2002, no. 6, p. 887.
12. Tsodikov, M.V., Bukhtenko, O.V., Slivinskii, E.V., Slastikhina, L.N., Voloshchuk, A.M., Kriventsov, V.V., and Kitaev, L.E., *Izv. Akad. Nauk, Ser. Khim.*, 2000, no. 11, p. 1829.
13. Tsodikov, M.V., Slivinskii, E.V., Yushchenko, V.V., Kitaev, L.E., Kriventsov, V.V., Kochubei, D.I., and Teleshev, A.T., *Izv. Akad. Nauk, Ser. Khim.*, 2000, no. 12, p. 2037.
14. Yamaguchi, K., Ebitani, K., Yoshida, T., Yoshida, H., and Kaneda, K., *J. Am. Chem. Soc.*, 1999, vol. 121, p. 4526.
15. Teleshev, A.T., Vasil'eva, L.N., Nifant'ev, E.E., Tsodikov, M.V., Bukhtenko, O.V., and Zhdanova, T.N., in *Aktual'nye problemy neftekhimii* (Topical Problems of Petroleum Chemistry), Moscow, 2001, p. 106.
16. Gansaüer, A., Barchuk, A., Keller, F., Schmitt, M., Grimme, S., Gerenkamp, M., Mück-Lichtenfeld, C., Daasbjerg, K., and Svith, H., *J. Am. Chem. Soc.*, 2007, vol. 129, p. 1359.
17. Di Serio, M., Iengo, P., Gobetto, R., Bruni, S., and Santacesaria, E., *J. Mol. Catal. A: Chem.*, 1996, vol. 112, p. 235.
18. Improta, R., Di Serio, M., and Santacesaria, E., *J. Mol. Catal. A: Chem.*, 1999, vol. 137, p. 169.
19. Maihom, T., Namuangruk, S., Nanok, T., and Limtrakul, J., *J. Phys. Chem. C*, 2008, vol. 112, p. 12914.
20. Granovsky, A.A., *Firefly Version 7.1.G.* http://classic.chem.msu.su/gran/firefly/inde.html
21. Parr, R.G. and Yang, W., *Density-Functional Theory of Atoms and Molecules*, New York: Oxford Univ. Press, 1989.
22. Becke, A.D., *Phys. Rev. A: At. Mol. Opt. Phys.*, 1986, vol. 33, p. 2786.
23. Becke, A.D., *J. Chem. Phys.*, 1993, vol. 98, p. 5648.
24. Lee, C., Yang, W., and Parr, R.G., *Phys. Rev. B: Condens. Matter*, 1988, vol. 37, p. 785.
25. Hehre, W.J., Ditchfield, R., and Pople, J.A., *J. Chem. Phys.*, 1972, vol. 56, p. 2257.
26. Hariharan, P.C. and Pople, J.A., *Theor. Chim. Acta*, 1973, vol. 28, p. 213.
27. Francl, M.M., Petro, W.J., Hehre, W.J., Binkley, J.S., Gordon, M.S., DeFrees, D.J., and Pople, J.A., *J. Chem. Phys.*, 1982, vol. 77, p. 3654.
28. Rassolov, V., Pople, J.A., Ratner, M., and Windus, T.L., *J. Chem. Phys.*, 1998, vol. 109, p. 1223.
29. Stevens, W.J., Basch, H., and Krauss, M., *J. Chem. Phys.*, 1984, vol. 81, p. 6026.
30. Stevens, W.J., Basch, H., Krauss, M., and Jasien, P., *Can. J. Chem.,* 1992, vol. 70, p. 612.
31. Cundari, T.R. and Stevens, W.J., *J. Chem. Phys.*, 1993, vol. 98, p. 5555.
32. Hirshfeld, F., *Theor. Chim. Acta*, 1977, vol. 44, p. 129.
33. Glendening, E.D., Badenhoop, J.K., Reed, A.E., Carpenter, J.E., Bohmann, J.A., Morales, C.M., and Weinhold, F., *NBO 5.0*, Madison: Theoretical Chemistry Inst., Univ. of Wisconsin, 2001.
34. Zhurko, G.A., ChemCraft. http://www.chemcraftprog.com

35. Mattioli, G., Filippone, F., Alippi, P., and Amore Bonapasta, A., *Phys. Rev. B: Condens. Matter*, 2008, vol. 78, p. 241201(R).
36. Mikheeva, E.P., Kachurovskaya, N.A., and Zhidomirov, G.M., *Kinet. Catal.*, 2002, vol. 43, p. 223.
37. Lazzeri, M. and Selloni, A., *Phys. Rev. Lett.*, 2001, vol. 87, pp. 266105–1.
38. Nakomoto, K., *Infrared and Raman Spectra of Inorganic and Coordination Compounds*, New York: Wiley, 1986, 4th ed.
39. Bellamy, L.J., *The Infra-Red Spectra of Complex Molecules*, London: Methuen, 1959.
40. Li, F., Jiang, Y., Xia, M., Sun, M., Xue, B., Liu, D., and Zhang, X., *J. Phys. Chem. C*, 2009, vol. 113, p. 18134.
41. Guerrero, G., Mutin, P.H., and Vioux, A., *Chem. Mater.*, 2001, vol. 13, p. 4367.
42. Yu, J.C., Zhang, L., Zheng, Z., and Zhao, J., *Chem. Mater.*, 2003, vol. 15, p. 2280.
43. Lin, L., Lin, W., Xie, J.L., Zhu, Y.X., Zhao, B.Y., and Xie, Y.C., *Appl. Catal., B*, 2007, vol. 75, p. 52.
44. Samantaray, S.K. and Parida, K.M., *J. Mater. Sci.*, 2003, vol. 38, p. 1835.
45. Körösi, L. and Dékány, I., *Colloids Surf., A*, 2006, vol. 280, p. 146.
46. Körösi, L., Papp, S., Bertóti, I., and Dékány, I., *Chem. Mater.*, 2007, vol. 19, p. 4811.
47. Bhaumik, A. and Inagaki, S., *J. Am. Chem. Soc.*, 2001, vol. 123, p. 691.
48. Corbridge, D.E.C. and Lowe, E.J., *J. Chem. Soc.*, 1954, p. 493.
49. Bergmann, E.D., Littauer, U.Z., and Pinchas, S., *J. Chem. Soc.*, 1952, p. 847.
50. Davydov, A.A., *IK-spektroskopiya v khimii poverkhnosti okislov* (IR Spectroscopy Applied to the Chemistry of Oxide Surfaces), Novosibirsk: Nauka, 1984.
51. Primet, M., Pichat, P., and Mathieu, M.-V., *J. Phys. Chem.*, 1971, vol. 75, p. 1216.
52. Parfitt, G.D., *Prog. Surf. Membr. Sci*, 1976, vol. 11, p. 181.
53. Ignatchenko, A., Nealon, D.G., Dushane, R., and Jumphries, K., *J. Mol. Catal. A: Chem.*, 2006, vol. 256, p. 57.
54. Diebold, U., *Surf. Sci. Rep.*, 2003, vol. 48, p. 53.
55. Hadjiivanov, K.I. and Klissurski, D.G., *Chem. Soc. Rev.*, 1996, vol. 25, p. 61.
56. Busca, G., Lorenzelli, V., Galli, P., La Ginestra, A., and Patrono, P., *J. Chem. Soc., Faraday Trans. 1*, 1987, vol. 83, p. 853.
57. Busca, G., Cavani, F., Centi, G., and Trifiro, F., *J. Catal.*, 1986, vol. 99, p. 400.
58. Hadjiivanov, K.I., Klissurski, D.G., and Davydov, A.A., *J. Catal.*, 1989, vol. 116, p. 498.